Ontogeny and function of the circadian clock in intestinal organoids

Andrew E Rosselot[1,†], Miri Park[1,†], Mari Kim[1,†], Toru Matsu-Ura[1] (iD), Gang Wu[2], Danilo E Flores[2], Krithika R Subramanian[1], Suengwon Lee[1], Nambirajan Sundaram[3], Taylor R Broda[4], Heather A McCauley[4], Jennifer A Hawkins[3], Kashish Chetal[5], Nathan Salomonis[5], Noah F Shroyer[6] (iD), Michael A Helmrath[3,4], James M Wells[4,7], John B Hogenesch[2,8], Sean R Moore[9,*] (iD) & Christian I Hong[1,4,8,10,**] (iD)

Abstract

Circadian rhythms regulate diverse aspects of gastrointestinal physiology ranging from the composition of microbiota to motility. However, development of the intestinal circadian clock and detailed mechanisms regulating circadian physiology of the intestine remain largely unknown. In this report, we show that both pluripotent stem cell-derived human intestinal organoids engrafted into mice and patient-derived human intestinal enteroids possess circadian rhythms and demonstrate circadian phase-dependent necrotic cell death responses to *Clostridium difficile* toxin B (TcdB). Intriguingly, mouse and human enteroids demonstrate anti-phasic necrotic cell death responses to TcdB. RNA-Seq analysis shows that ~3–10% of the detectable transcripts are rhythmically expressed in mouse and human enteroids. Remarkably, we observe anti-phasic gene expression of *Rac1*, a small GTPase directly inactivated by TcdB, between mouse and human enteroids, and disruption of *Rac1* abolishes clock-dependent necrotic cell death responses. Our findings uncover robust functions of circadian rhythms regulating clock-controlled genes in both mouse and human enteroids governing organism-specific, circadian phase-dependent necrotic cell death responses, and lay a foundation for human organ- and disease-specific investigation of clock functions using human organoids for translational applications.

Keywords circadian rhythms; *Clostridium difficile* toxin B; human enteroids; intestinal organoids; *Rac1*

Introduction

3-dimensional (3D) organoids are multicellular *in vitro* model systems possessing *in vivo* tissue architecture and function that is unattainable in homogenous single cell culture systems. Multiple tissues have been generated as organoids from a range of sources including pluripotent stem cells (PSC) and patient biopsies (Clevers, 2016). The source utilized for organoid generation influences the maturity of the end sample. For example, PSCs are differentiated through distinct developmental stages, definitive endoderm (DE) and midgut tube formation (MG), to generate human intestinal organoids (HIOs) (Fig 1A and B), a process mimicking the blastocyst, gastrula, somite, and fetal stages of intestinal development, respectively (Spence *et al*, 2011; Wells & Spence, 2014). The fetal nature of HIOs is highlighted by the absence of a full spectrum of markers for mature epithelial cell types (Watson *et al*, 2014; Finkbeiner *et al*, 2015). HIOs can be matured beyond their fetal stage by surgical implantation into the kidney capsule of immunocompromised non-obese diabetic (NOD) *scid* gamma (NSG) mice. When transplanted, they become vascularized by the host circulatory system and

1   Department of Pharmacology & Systems Physiology, University of Cincinnati, Cincinnati, OH, USA
2   Division of Human Genetics and Immunobiology, Center for Chronobiology, Department of Pediatrics, Cincinnati Children's Hospital Medical Center, Cincinnati, OH, USA
3   Department of Pediatric Surgery, Cincinnati Children's Hospital Medical Center, Cincinnati, OH, USA
4   Center for Stem Cell and Organoid Medicine, Division of Developmental Biology, Cincinnati Children's Hospital Medical Center, Cincinnati, OH, USA
5   Division of Biomedical Informatics, Cincinnati Children's Hospital Medical Center, Cincinnati, OH, USA
6   Gastroenterology and Hepatology, Baylor College of Medicine, Houston, TX, USA
7   Division of Endocrinology, Cincinnati Children's Hospital Medical Center, Cincinnati, OH, USA
8   Center for Chronobiology, Cincinnati Children's Hospital Medical Center, Cincinnati, OH, USA
9   Division of Pediatric Gastroenterology, Hepatology, and Nutrition, Department of Pediatrics, University of Virginia School of Medicine, Charlottesville, VA, USA
10 Division of Developmental Biology, Cincinnati Children's Hospital Medical Center, Cincinnati, OH, USA
    *Corresponding author. Tel: +1 434 924 7749; E-mail: sean.moore@virginia.edu
    **Corresponding author. Tel: +1 513 558 5093; E-mail: christian.hong@uc.edu
    †These authors contributed equally to this work

develop a well-defined crypt-villus architecture. Transcriptome-wide hierarchical clustering shows that transplanted samples are matured to an intermediate state between HIOs and adult intestinal tissue, containing a wider range of intestinal cell type markers compared to HIOs but not equivalent to adult intestinal tissue (Finkbeiner *et al*, 2015). Intestinal crypts from the transplanted human tissue can be isolated and cultured *in vitro* to generate mouse kidney capsule-matured human intestinal enteroids (kcHIEs; Fig 1A). Analogously, crypts from human intestinal biopsies can be isolated and grown *in vitro* to generate biopsy-derived HIEs (bHIEs; Mahe *et al*, 2015) (Fig 1A). Recent progress highlights the versatile utility of the organoid and enteroid model systems to investigate numerous complex biological questions including the molecular mechanisms maintaining the intestinal stem cell niche (Kretzschmar & Clevers, 2016), host–pathogen interactions (Forbester *et al*, 2015), cellular development (Sinagoga *et al*, 2018), and non-pathogenic bacteria interactions (Hill *et al*, 2017). However, the development and physiological functions of circadian rhythms in human intestinal organoids/enteroids have not been investigated. In this report, we investigated the development of circadian rhythms from PSCs to kcHIEs and utilized bHIEs and mouse enteroids to characterize clock-controlled genes (CCGs) and circadian functions in both mouse and human intestinal epithelium.

Circadian rhythms exist throughout the body, providing temporal information to biological processes ranging from metabolism to cell proliferation. Molecularly, circadian rhythms are governed by a transcriptional–translational feedback loop (TTFL), which generates robust circadian oscillations at the single cell level (Nagoshi *et al*, 2004). Two basic helix–loop–helix (bHLH) PER-ARNT-SIM (PAS) domain containing proteins, CLOCK (circadian locomotor output cycles kaput) and BMAL1 (brain and muscle Arnt-like protein-1), form a heterodimeric circadian transcription factor that recognizes E-box motifs on target gene promoters including *Period (Per1, Per2, Per3)* and *Cryptochrome (Cry1, Cry2)*. PER and CRY bind together in the cytoplasm (Schmalen *et al*, 2014) and translocate into the nucleus where they interact with the CLOCK-BMAL1 heterodimer to repress its activity (Lee *et al*, 2001). PER and CRY are then ubiquitinated and degraded, relieving CLOCK-BMAL1 from negative feedback to re-initiate the cycle (Reischl *et al*, 2007; Siepka *et al*, 2007; Yoo *et al*, 2013). CLOCK-BMAL1 forms additional feedback loops with nuclear orphan receptor transcription factors. CLOCK-BMAL1 drive rhythmic expression of positive (*Rorα, Rorβ, Rorγ*) and negative (*Rev-erbα, Rev-erbβ*) nuclear receptors that feedback on *Bmal1* by competitively binding at ROR response elements (RORE) on the *Bmal1* promoter (Preitner *et al*, 2002; Sato *et al*, 2004; Guillaumond *et al*, 2005).

The suprachiasmatic nucleus (SCN) is commonly referred to as the "master clock" of the mammalian system. Located in the hypothalamus, the SCN contains approximately 20,000 neurons that process photic signals to coordinate circadian rhythms in peripheral organs to external light/dark signals (Pando *et al*, 2002; Schibler *et al*, 2015). However, peripheral clocks are malleable and can be dissociated from SCN coordination by non-photic circadian zeitgebers. For example, mice restricted to food during their inactive period (i.e., light phase or subjective day) realign the phase of clock and metabolic genes in the liver, but not SCN, to coincide with food availability (Damiola *et al*, 2000). Intriguingly, the intestinal microbiota changes over a circadian cycle (Thaiss *et al*, 2014), and perturbation of the microbiome may impact the function of peripheral circadian rhythms. Antibiotic-induced depletion of microbiota induces constitutively high expression of *Rev-erbα* that abolishes rhythmic Toll-like receptor (TLR) expression (Mukherji *et al*, 2013). Loss of microbiota was also shown to change rhythmic gene expression within the mouse intestinal transcriptome while leaving behavioral rhythms intact (Thaiss *et al*, 2016). Notably, the recent development of tissue-specific conditional *Bmal1* rescue mice was instrumental in uncovering intact peripheral circadian rhythms in the skin epidermis and liver in the absence of circadian signaling from the SCN (Welz *et al*, 2019). These data highlight the importance of peripheral clocks and their ability to process input signals from local factors. More work is needed to uncover fundamental understanding of the conditions and mechanisms that integrate and dissociate the master and peripheral clocks. In this report, we utilized human intestinal organoids and enteroids to characterize the robustness of circadian rhythms during the development of intestinal tissue and investigated the functional role of the intestinal circadian clock in response to *Clostridium difficile* toxin B (TcdB) highlighting a critical function of the endogenous intestinal circadian clock.

Clostridium difficile is a spore-forming, gram-positive, toxin-producing intestinal pathogen. *C. diff.* infection (CDI) manifests with diarrhea symptoms that can progress into pseudomembranous colitis and toxic megacolon (Kelly *et al*, 1994; Buffie *et al*, 2012). CDI pathogenesis includes the luminal release of two toxins, toxin A (TcdA) and B (TcdB), that bind to intestinal cellular receptors (Chen *et al*, 2018) and enter the cell via endocytosis (Papatheodorou *et al*, 2010). In the cytoplasm, autocatalytic cleavage releases the catalytic glucosyltransferase domain of the toxins (Reineke *et al*, 2007) that inactivate the small GTPases RHOA, RAC1, and CDC42, resulting in cellular cytoskeleton breakdown, disruption of epithelial barrier function, and cell death (Just *et al*, 1995; Abt *et al*, 2016). In addition, the NOX1 NADPH oxidase complex has also been implicated in promoting toxin-mediated cell death at high concentrations of TcdB (Farrow *et al*, 2013). Several experimental models have been utilized to investigate *C. difficile* pathogenesis and each present

---

Figure 1. Maturation of HIOs is required for the development of robust circadian rhythms.

A   Schematic summary for establishing 3D *in vitro* human intestinal organoids (HIOs—grey), kidney capsule matured human intestinal enteroids (kcHIEs—red), biopsy-derived human intestinal enteroids (bHIEs—blue) or mouse enteroids (yellow).

B   Raw (top) and detrended (bottom) *Bmal1-luc* bioluminescence data throughout directed differentiation of PSCs to HIOs, kcHIEs, and bHIEs.

C   Period length decreases with continual differentiation of PSCs into HIOs. Maturation of HIOs into kcHIEs leads to 24-hour rhythms with greater reproducibility.

D   The amplitude of oscillations is significantly higher in kcHIEs/bHIEs compared to HIOs. *Bmal1-luc* traces in B were generated by plotting the standard deviation of $n \geq 3$ biological replicates.

Data information: Panels (C and D) depict mean ± S.D. of $n \geq 3$ biological replicates. AU stands for arbitrary units.
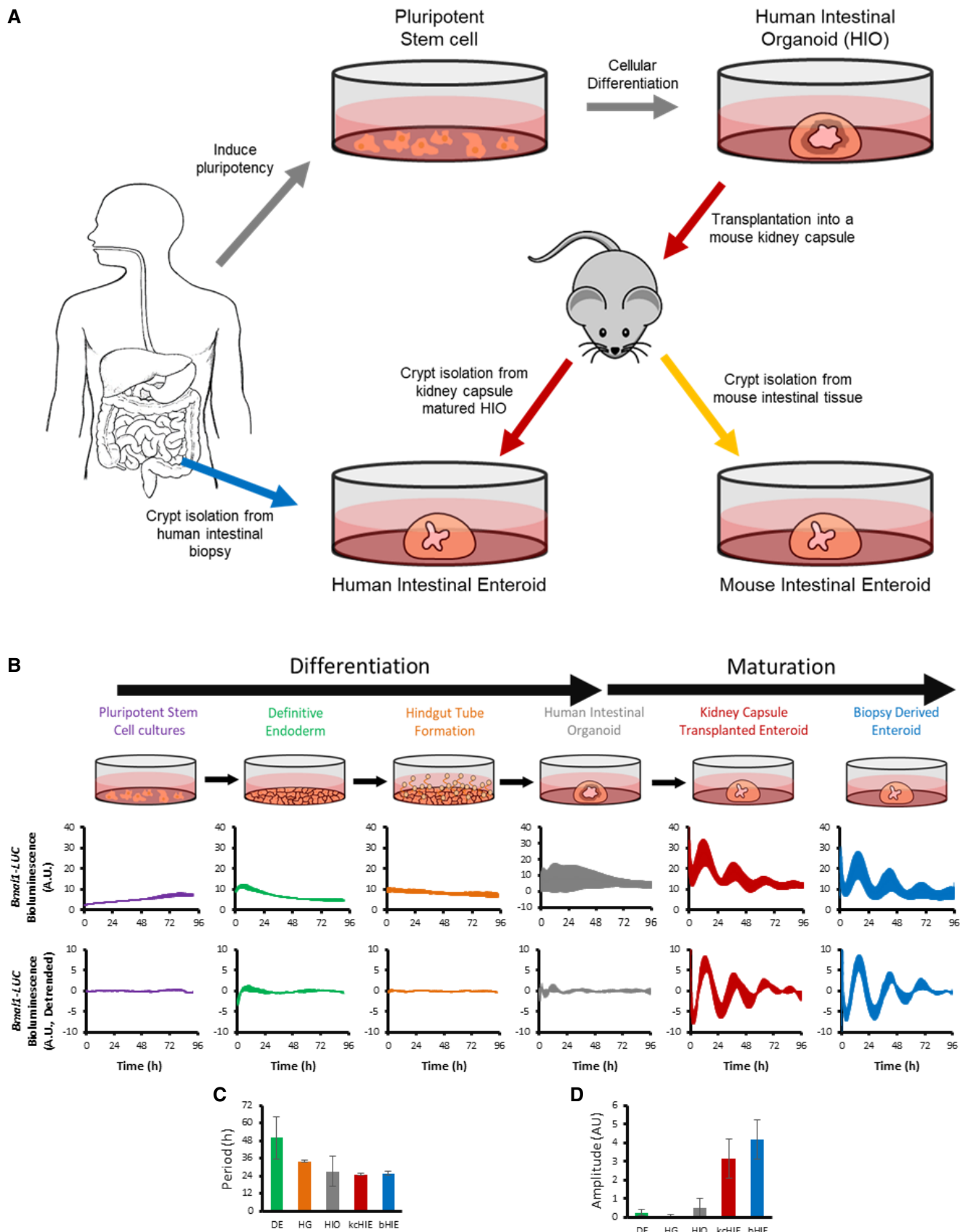Source data are available online for this figure.

Figure 1.

limitation. *In vivo* rodent studies have been associated with low reproducibility attributed to confounding variables such as different *C. diff.* strains, antibiotic regimen to induce susceptibility, and cross contamination of animal housing (Best *et al*, 2012). The translatability of pathophysiological findings from rodent models to humans also cannot be guaranteed. *In vitro* and *ex vivo* studies are, comparatively, controllable but lack multicellular complexity or multi-time point scalability, respectively. Human intestinal organoids/enteroids offer an opportunity to overcome these limitations by coupling *in vitro* experimental control with recapitulation of an *in vivo* human intestinal epithelium. 3D intestinal cultures have been successfully utilized to gain insights into the pathogenic response to human rotavirus (Saxena *et al*, 2016), *E. coli (*Noel *et al*, 2017*),* and *Clostridium difficile* toxins A/B (Leslie *et al*, 2015). These studies, however, did not investigate the influence of the circadian clock in the pathogenic response. Circadian clock-mediated time of day dependency in the pathogenesis of *Salmonella* Typhimurium (Bellet *et al*, 2013) and herpes simplex virus (Edgar *et al*, 2016) has been observed in mice, but it is unknown whether humans show identical circadian time-dependent responses via conserved molecular mechanisms. In this report, we utilized mouse and human intestinal enteroids to uncover potential differences with respect to circadian phase-dependent necrotic cell death responses to TcdB.

Results

The development of a robust intestinal circadian clock requires maturation of HIOs

Mouse embryonic stem cells (ESC) do not possess circadian rhythms and have low expression of several canonical clock genes in comparison to NIH3T3 cells (Kowalska *et al*, 2010). Retinoic acid-induced differentiation of mouse embryonic stem cells initiates autonomous circadian oscillations while reverting differentiated cells back to an induced pluripotent stem cell (iPSC) state abolishes circadian rhythms (Yagita *et al*, 2010). Subsequent studies revealed that during the early stages of cellular differentiation, PER1/PER2 are sequestered in the cytoplasm (Umemura *et al*, 2014) and the expression of CLOCK is downregulated by *Dicer/Dgcr8*-dependent post-transcriptional regulation of *Clock* mRNA (Umemura *et al*, 2017) disrupting autonomous oscillations of circadian rhythms. Identical to mouse ESCs and iPSCs, human ESCs and iPSCs lack circadian rhythms and show post-transcriptional suppression of CLOCK protein expression (Dierickx *et al*, 2017; Umemura *et al*, 2019). Terminally differentiated cardiomyocytes from human ESCs demonstrate rhythmic gene regulation of CCGs, which regulate circadian time-dependent responses to doxorubicin (Dierickx *et al*, 2017). Based on these data, we hypothesized that developmental maturation is a critical process for the development of robust circadian rhythms in 3D multicellular intestinal organoids.

To investigate the development of circadian rhythms in multicellular organoids, activity of circadian rhythms was assessed at different stages of development of human intestinal organoids and enteroids using *Bmal1-luciferase* (*Bmal1-luc*) reporter (Fig 1B). iPSCs were stably transduced with a plasmid containing *Bmal1-luc* using lentivirus (Brown *et al*, 2005) and differentiated through two distinct stages: definitive endoderm (DE) and midgut tube (MG)

formation (Spence *et al*, 2011). *Bmal1-luc* reporter activity was recorded throughout differentiation with a luminometer (Kronos-DIO™, ATTO). In agreement with previous reports (Umemura *et al*, 2019), iPSCs did not show circadian oscillations (Fig 1B (purple), Fig EV1A). Interestingly, we observe low-intensity bioluminescence signals with long period lengths of about 50 and 34 h at the DE and MG stages, respectively (Fig 1B (green and orange), Fig EV1B and C). On the other hand, HIOs that were stably transduced with *Bmal1-luc* plasmids demonstrated circadian oscillations with low bioluminescence output (Figs 1B (grey) and Fig EV1D). These data show that differentiation of iPSCs into multicellular HIOs promotes period length shortening, culminating with 24-hour bioluminescent oscillations in HIOs (Fig 1C and D). However, circadian oscillations in these HIOs are not robust, lacking phase uniformity between independent experiments and unable to maintain oscillations longer than 48 h post-synchronization of circadian rhythms (Figs 1B and EV1D). Although HIOs contain multiple intestinal epithelial cell types (Spence *et al*, 2011), they do not possess the full spectrum of epithelial cell markers, which reflect their immature, fetal-like state. The stem and Paneth cell markers, *Lgr5* and *Lysozyme*, respectively, are expressed in both HIOs and human tissue (Finkbeiner *et al*, 2015). The expression of secondary stem cell (*Olfm4*) and Paneth cell (*Dll4*, *Reg3a*) markers are, however, attenuated in HIOs, indicating they do not possess matured intestinal epithelial cell types (Finkbeiner *et al*, 2015) (Fig EV2A and B). Therefore, we transplanted HIOs into the kidney capsule of NSG mice and allowed them to mature over 3-months (Watson *et al*, 2014) to test if maturation of HIOs could enhance the robustness of circadian rhythms.

After 3 months of maturation, human intestinal crypts were isolated from the grafts to establish *in vitro* mouse kidney capsule-matured human intestinal enteroids (kcHIEs; Mahe *et al*, 2015) (Fig 1A). In addition, we generated biopsy-derived human intestinal enteroids (bHIEs) to compare circadian rhythms from matured human samples with HIOs and kcHIEs (Fig 1A). Both kcHIEs and bHIEs were transduced with the *Bmal1-luc* plasmid and tested for rhythmic bioluminescent output. In contrast to HIOs, kcHIEs and bHIEs demonstrated robust circadian oscillations, demonstrated by sustained high amplitude oscillations of bioluminescent output from *Bmal1-luc* reporter (Fig 1B). To validate the above bioluminescent data, we performed time course experiments collecting HIOs, kcHIEs, and bHIEs every 4 h over two circadian cycles for real-time quantitative reverse transcription polymerase chain reaction (qRT–PCR). The expression of *Bmal1*, *Rev-erbα*, and *Per2* was significantly reduced and arrhythmic in HIOs (Fig 2A). In contrast, both kcHIEs and bHIEs demonstrated circadian rhythms with appropriate phase relationships between positive (*Bmal1*) and negative (*Per2*, *Rev-erbα*) clock elements (Fig 2B and C). The average expression of these genes are not significantly different between kcHIEs and bHIEs except for *Rev-erbα* (Fig 2D). Interestingly, the average amplitude of *Bmal1*, *Per2*, and *Rev-erbα* are significantly lower in kcHIEs compared to bHIEs (Fig 2E), which suggest that bHIEs possess a more robust circadian clock compared to kcHIEs. Based on these data, we hypothesize that circadian time-dependent responses to external perturbations will be observed in kcHIEs and bHIEs, but not in HIOs. As a proof of principle, we tested the circadian clock-dependent response to *Clostridium difficile* toxin B (TcdB).

The intestinal circadian clock in mouse and human enteroids regulate circadian phase-dependent necrotic cell death responses to TcdB

Circadian clock-dependent time-of-day variation in the pathogenic response has been demonstrated for *Salmonella enterica serovar* Typhimurium (Bellet *et al*, 2013), herpes and influenza A virus (Edgar *et al*, 2016) and *Leishmania*, in mice (Kiessling *et al*, 2017). However, circadian clock-dependent responses to bacterial toxins in mouse or human enteroids have not been tested. It is critical to determine circadian clock-dependent responses to different external perturbations (e.g., pathogens, toxins, and nutrients) in both mouse and human enteroids to compare and contrast their responses in order to develop potential translational applications using patient-derived HIEs while taking advantage of various tools in transgenic mice. Therefore, we assessed circadian clock-dependent responses following exposure to purified TcdB in both mouse and human enteroids.

Mouse enteroids were isolated from the tamoxifen-inducible *Bmal1^{f/f}-EsrCRE* mouse (Yang *et al*, 2016). *In vitro* treatment of tamoxifen in *Bmal1^{f/f}-EsrCRE* enteroids successfully abolished circadian rhythms in contrast to control enteroids (Fig EV3A–D), which enabled us to use *Bmal1-floxed* enteroids as arrhythmic-negative controls. Circadian rhythms of *Bmal1^{f/f}-EsrCRE* enteroids were synchronized using dexamethasone, and 10 ng/ml of TcdB was added to the growth media at 24- (T24) and 36-h (T36) post-dexamethasone treatment (Fig EV4A). SYTOX^{TM} Orange, a fluorescent dye that stains nucleic acids in cells with disrupted membranes, was added simultaneously with TcdB to quantify necrotic cell death at 2, 24, and 48 h post-exposure of TcdB. In control *Bmal1^{f/f}-EsrCRE* enteroids, without tamoxifen treatments, we observe greater necrotic cell death in the T36 group compared to T24 at 48 h post-TcdB treatments (Fig 3A and B). Identical data were observed in mouse enteroids derived from PER2::LUC mice (Fig EV4B and C). In contrast, tamoxifen-treated *Bmal1-floxed* enteroids showed a loss of circadian time-dependent necrotic cell death responses to TcdB (Fig 3C and D), which indicates that the intestinal circadian clock regulates the observed circadian phase-dependent phenotypes. Next, we used the aforementioned three human organoid models to test whether this phenotype from mouse enteroids is conserved in human organoids.

HIOs, kcHIEs, and bHIEs were tested for circadian clock phase-dependent responses following the same protocol used for mouse enteroids. HIOs showed identical necrotic cell death responses between the T24 and T36 groups (Fig 4A and B) consistent with their lack of robust circadian rhythms (Fig 1B). In contrast, both kcHIEs and bHIEs demonstrated circadian phase-dependent necrotic cell death responses to TcdB with greater amount of cell death in the T24 compared to the T36 group for both kcHIEs and bHIEs (Fig 4C–F). These findings indicate that a functional, robust circadian clock is required for circadian phase-dependent responses to TcdB. Intriguingly, mouse and human enteroids demonstrated anti-phasic necrotic cell death responses to TcdB. Mouse enteroids showed a higher necrotic cell death in the T36 group (Fig 3B), whereas HIEs were more responsive in the T24 group (Fig 4D and F).

Necrotic cell death responses measured by SYTOX^{TM} Orange do not provide quantitative data. Therefore, we used fluorescence-activated cell sorting (FACS) analysis to measure both necrotic and apoptotic cells using propidium iodide and Annexin V, respectively (Natarajan *et al*, 2019), in mouse enteroids and bHIEs. Consistent with the results obtained with SYTOX^{TM} Orange, we observed anti-phasic necrotic cell death responses between mouse enteroids and bHIEs (Fig EV5A–C,F). In contrast, we did not observe circadian time-dependent changes in the number of apoptotic cells (Fig EV5D, E,G,H). We speculated that anti-phasic behavioral rhythms between diurnal humans and nocturnal mice could be hardwired within the peripheral circadian clocks determining distinct phases of CCGs between mouse and human enteroids. To uncover CCGs in HIEs and mouse enteroids and identify potential target genes for the observed anti-phasic necrotic cell death responses in mouse vs. human enteroids, we performed a 48-h time course experiment with 2-h resolution extracting RNA from bHIEs and mouse enteroids for RNA-Seq.

Approximately 3–10% of detectable transcripts in mouse and human intestinal enteroids show rhythmic gene expression

For the analysis of our RNA-Seq data, we used RAIN algorithm (Thaben & Westermark, 2014) to identify CCGs and performed phase set enrichment analysis (PSEA; Zhang *et al*, 2016) to determine signaling pathways that are under the control of intestinal circadian clocks. For RAIN analysis, we excluded low expressing transcripts with mean expression below the lowest 25%, and transcripts with null expression in more than 2/3 of the samples. Rhythm cutoff was set to RAIN BH *q*-value < 0.15. The analysis uncovered 445 and 1,728 CCGs out of 14,342 and 17,898 detectable transcripts, which are 3.1% and 9.6% of total genes above the cutoff, in mouse enteroids and bHIEs, respectively (Fig 5A). This is in sharp contrast to less than a dozen cycling genes in other *in vitro* systems (i.e., NIH3T3 and U2OS cells) (Hughes *et al*, 2009). Importantly, heatmap of Spearman's rho for circadian clock and clock-associated genes show appropriate correlation of each gene against the rest in both mouse and human intestinal enteroids (Fig 5B), which confirmed that the circadian clock machinery is intact and functional with proper phase relationships in these enteroids.

Figure 2. kcHIEs and bHIEs show circadian rhythms with appropriate phase relationships between canonical clock genes.

A–C mRNA expression of *Bmal1* (black), *Rev-erbα* (grey) and *Per2* (red) in HIOs (A), kcHIEs (B), and bHIEs (C).

D, E (D) Average expression of *Bmal1* (black), *Rev-erbα* (grey) and *Per2* (red) in HIO, kcHIE, and bHIE. (E) Amplitude of *Bmal1* (black), *Rev-erbα* (grey) and *Per2* (red). AU stands for arbitrary units.

Data information: The data in panels (A–C) are shown as mean (bold line) ± SD with replicates displayed as dashed lines. (D, E) Panels show mean ± SD of $n = 3$ biological replicates. *$P < 0.05$, **$P < 0.01$, ***$P < 0.001$ (Tukey's multiple comparison).
Source data are available online for this figure.
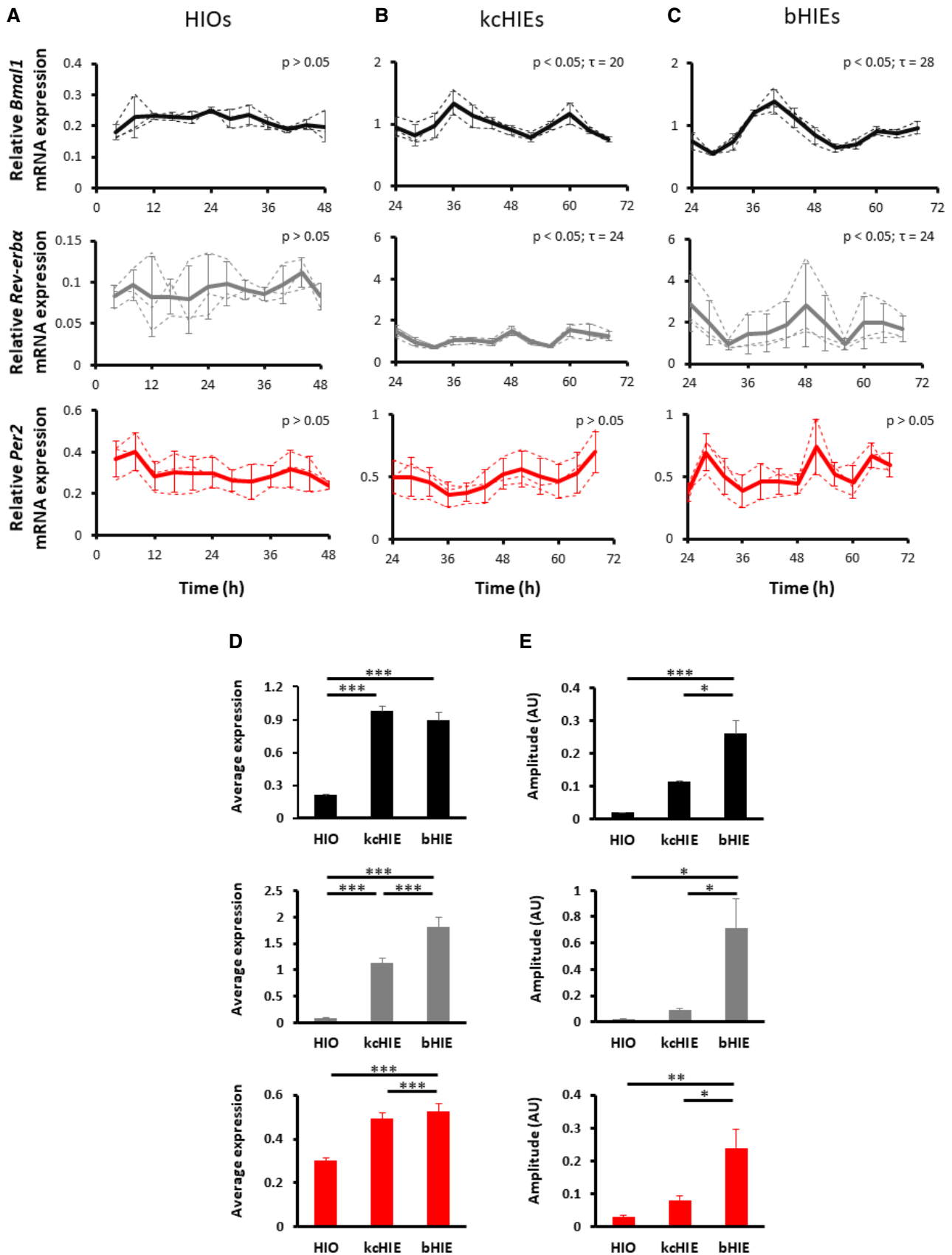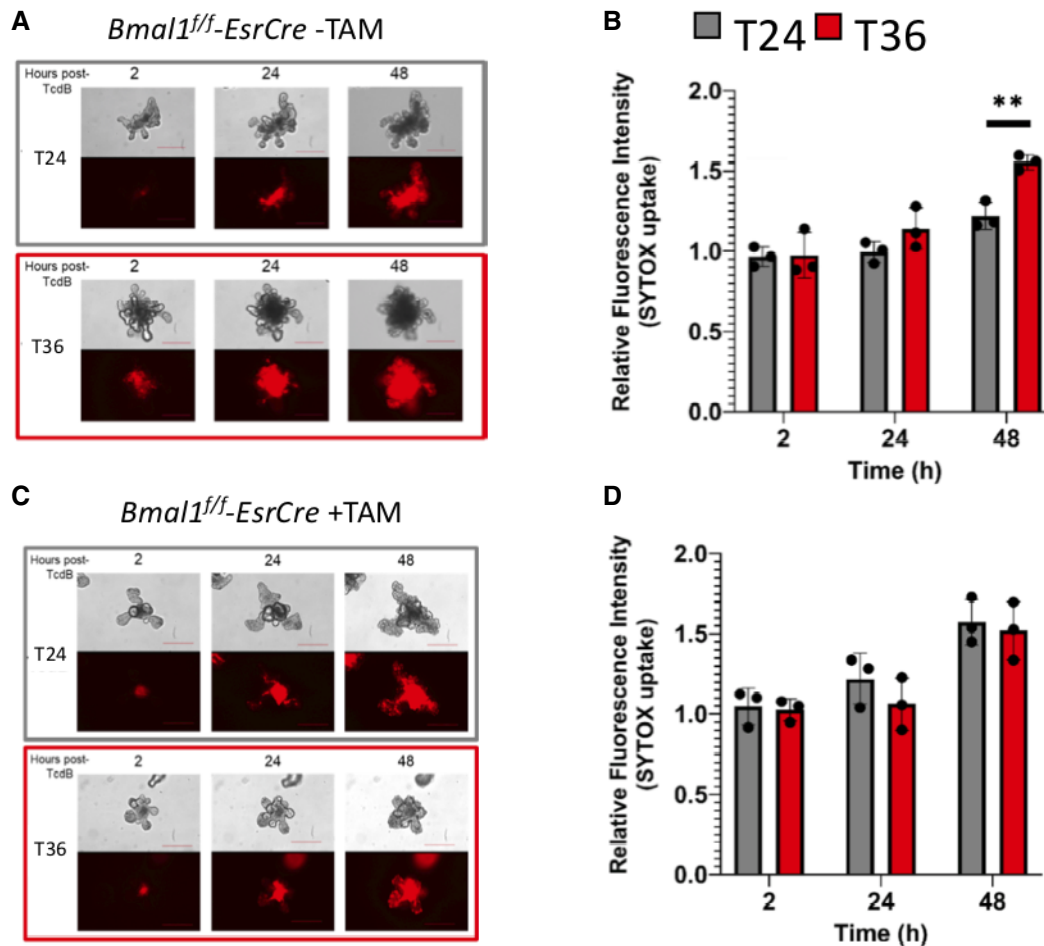
Figure 2.

Figure 3. Mouse enteroids show circadian phase-dependent necrotic cell death response to *Clostridium difficile* toxin B.

A   Representative images of necrotic cell death (SYTOX orange - red fluorescence) at 2-, 24- and 48 h post-exposure to 10 ng/ml TcdB in control *Bmal1^{f/f}-EsrCRE* enteroids. Scale bar = 250 μm.

B   Quantitative analysis of fluorescent intensity from SYTOX orange in control *Bmal1^{f/f}-EsrCRE* enteroids without tamoxifen treatment.

C   Representative images of necrotic cell death (SYTOX orange) at 2, 24, and 48 h post-exposure to 10 ng/ml TcdB in tamoxifen-treated circadian arrhythmic *Bmal1^{f/f}-EsrCRE* enteroids. Scale bar = 250 μm.

D   Quantitative analysis of fluorescent intensity from SYTOX orange in tamoxifen-treated circadian arrhythmic *Bmal1^{f/f}-EsrCRE* enteroids.

Data information: Data represented as mean ± SD of $n = 4$ biological replicates (i.e., enteroids derived from different mice). All of the data were normalized to time- and phase-matched vehicle controls set to 1. **$P < 0.01$ (two-way ANOVA).

Source data are available online for this figure.

Circadian time-dependent necrotic cell death responses may be due to rhythmic expression of TcdB receptor genes (i.e., *Cspg4*, *Pvrl3*, and *Fzd1,2,7*), TcdB-targeted small GTPases (i.e., *Rac1*, *Cdc42* and *RhoA*), and/or NOX1,2 NADPH oxidase complexes (i.e., *Nox1*, *Noxo1*, *Noxa1*, *p22*, *Nox2*, *p47*, *p67*, *p22*, and *p40*). RAIN algorithm did not detect rhythmicity in most of the above transcripts. Specifically, RAIN detected two (*Rac1* and *Nox1*) and three (*Cspg4*, *Rac1*, and *Noxo1*) cycling transcripts in mouse and human enteroids, respectively, identifying *Rac1* as the only conserved rhythmic transcript in this category (Table EV1, Appendix Fig S1A and B).

Phase set enrichment analysis uses prior knowledge to identify signaling pathways demonstrating temporally coordinated expression profiles. PSEA revealed that the intestinal epithelial circadian clocks regulate temporal organization of 8 conserved signaling pathways in both mouse and human intestinal enteroids including metabolism, cell cycle, and circadian clock (Fig 5C, Table EV1). Six out of eight signaling pathways including circadian rhythms showed similar phases between mouse and human enteroids. Intriguingly, two signaling pathways, cell–cell communication and neurotrophin signaling pathways, showed dramatically difference phases. To our surprise, these two signaling pathways included a single TcdB target gene, *Rac1*, which showed anti-phasic expression between human and mouse enteroids. Hence, we validated the anti-phasic expression of *Rac1* between mouse and human enteroids using qRT–PCR (Fig 6A, Appendix Fig S2A). We observe arrhythmic expression of *Rac1* in both HIOs and *Bmal1-floxed* mouse enteroids, which is consistent
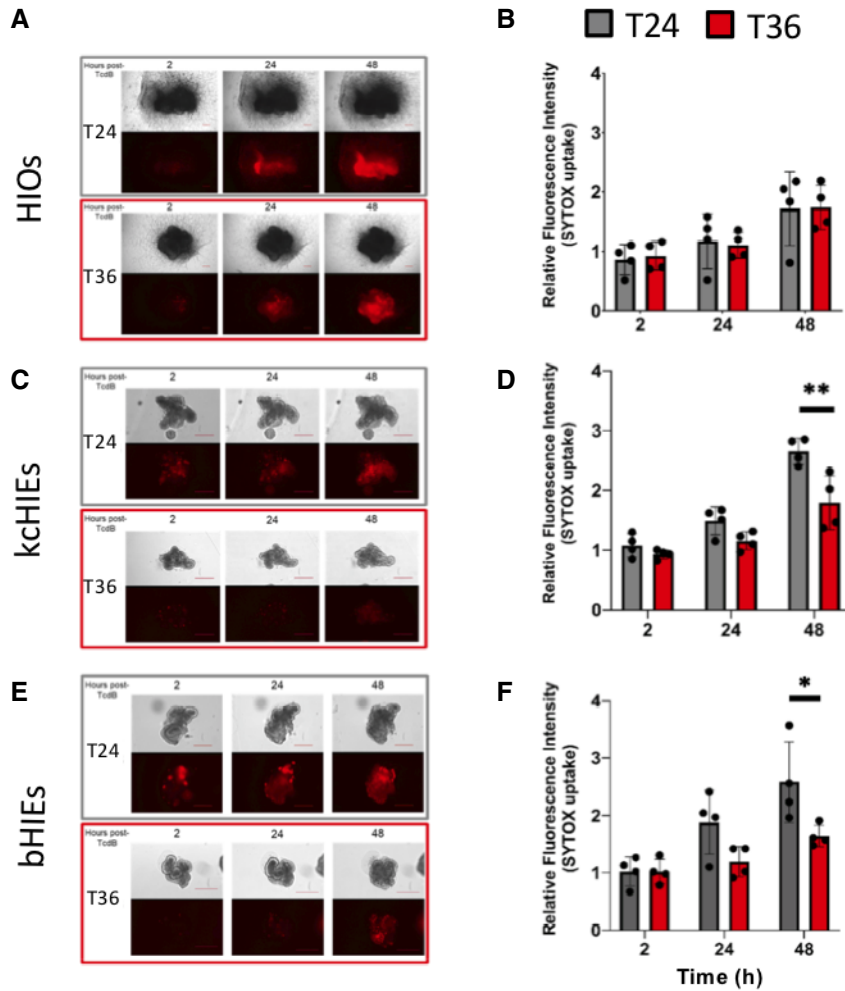
Figure 4. A functional circadian clock is needed for a circadian phase-dependent response to TcdB in human organoids.

A   Representative images of necrotic cell death (SYTOX orange) at 2, 24, and 48 h post-exposure to 0.1 μg/ml TcdB in HIOs. Scale bar = 250 μm.
B   Quantification of necrotic cell death in HIOs.
C   Representative images of necrotic cell death (SYTOX orange) at 2, 24, and 48 h post-exposure to 0.5 μg/ml TcdB in kcHIEs. Scale bar = 250 μm.
D   Quantification of necrotic cell death in kcHIEs.
E   Representative images of necrotic cell death (SYTOX orange) at 2, 24, and 48 h post-exposure to 0.5 μg/ml TcdB in bHIEs. Scale bar = 250 μm.
F   Quantification of necrotic cell death in bHIEs.

Data information: All samples were exposed to TcdB at two circadian time points, 24 h (T24, grey) or 36 h (T36, red) post-synchronization. Data are shown as mean ± SD of $n \geq 3$ biological replicates (i.e., HIOs are generated from different PSCs and bHIEs are derived from three different patients' samples). All data were normalized to time- and phase-matched vehicle controls set to 1. *$P < 0.05$, **$P < 0.01$ (two-way ANOVA).
Source data are available online for this figure.

with lack of circadian phase-dependent necrotic cell death responses (Appendix Fig S2B and C). Lastly, disruption of *Rac1* abolished circadian time-dependent necrotic cell death responses to TcdB in both mouse enteroids and bHIEs. We used *Rac1*-KD bHIEs and tamoxifen-inducible *Rac1*-KO mouse enteroids derived from *Rac1*[f/f]; CAGGCre-ER[TM] mice. Both *Rac1*-KO mouse enteroids and *Rac1*-KD bHIEs demonstrated a loss of circadian time-dependent necrotic cell death responses measured by SYTOX[TM] Orange (Fig 6B–D, Appendix Fig S3A–D). Together, our data strongly suggest that the rhythmic expression of *Rac1* determines the observed anti-phasic necrotic cell death response against TcdB in mouse vs. human enteroids.

Discussion

Circadian rhythms regulate CCGs in a tissue-specific manner throughout the body (Ruben *et al*, 2018). Circadian rhythms in peripheral organs are affected by numerous inputs including light (Buhr *et al*, 2019; Nayak *et al*, 2020), nutrients (Damiola *et al*, 2000; Stokkan *et al*, 2001; Crosby *et al*, 2019), and systemic cues from SCN (Silver *et al*, 1996; Guo *et al*, 2005; Barca-Mayo *et al*, 2017; Brancaccio *et al*, 2017; Tso *et al*, 2017). Previous studies characterizing CCGs in different organs from *in vivo* mice uncovered organ-specific regulation of circadian rhythms integrated by both peripheral clocks and systemic cues from SCN. Recent development of
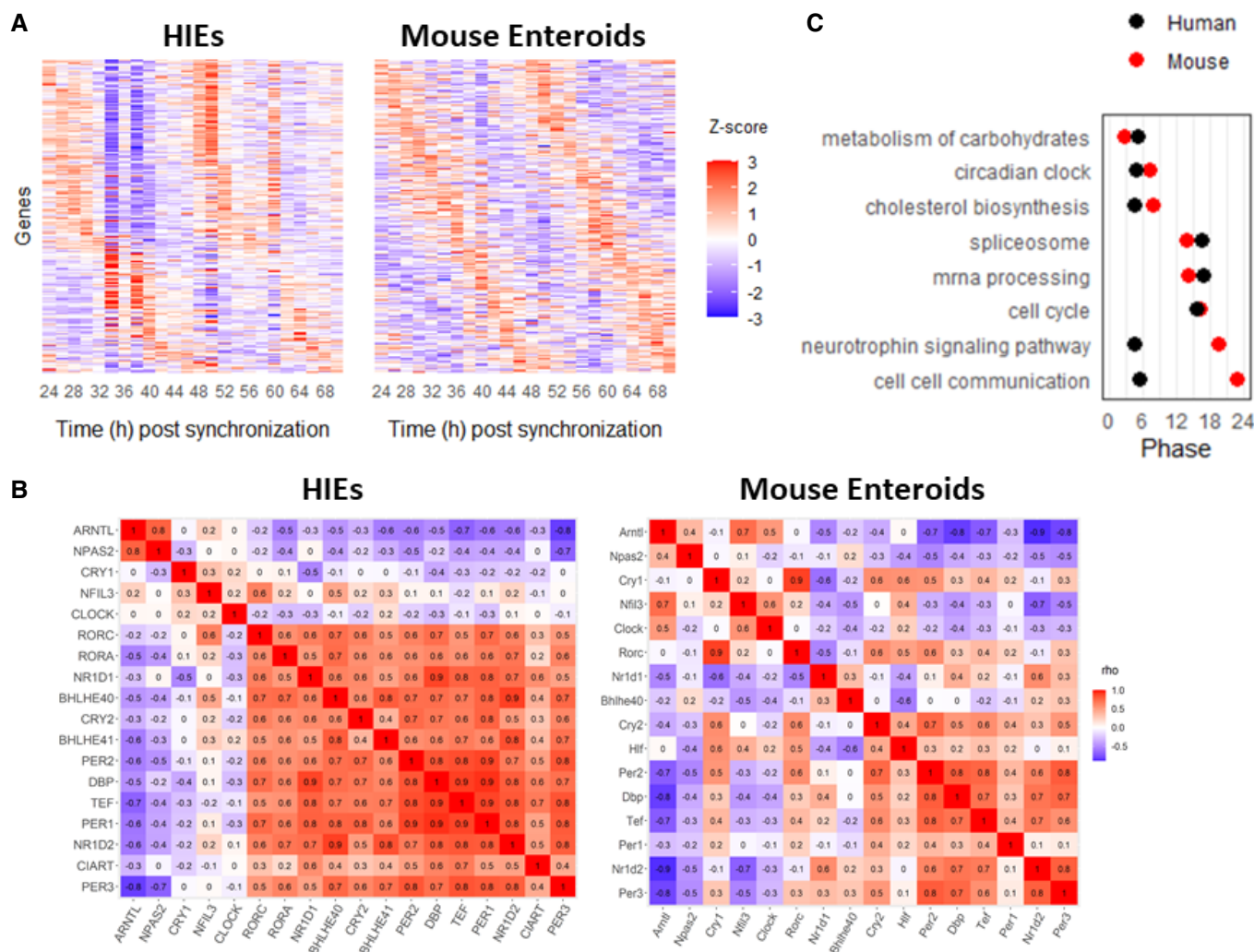
Figure 5. 3–10% of transcripts show circadian oscillations in mouse and human enteroids.

A   Heatmap of circadian transcripts over 48 h in mouse and human enteroids.
B   Spearman's rho for circadian clock and clock-associated genes.
C   8 conserved rhythmic signaling pathways identified by phase set enrichment analysis (PSEA).

Source data are available online for this figure.

tissue-specific conditional *Bmal1* rescue mice will be instrumental to discover organ-specific endogenous CCGs independent of SCN (Welz *et al*, 2019; Sinturel *et al*, 2021). Characterization of organ-specific endogenous CCGs is necessary to systematically compare and contrast changes of circadian gene expression profiles in the presence of systemic and external cues, and control and disease states (e.g., cancer). However, the discovery of organ-specific endogenous CCGs in humans is difficult, creating a major bottleneck hindering organ- and disease-specific investigation of circadian rhythms and CCGs for translational applications.

Human organoids are complex, multicellular *in vitro* systems that are devoid of systemic signaling factors, making them an appealing system to evaluate endogenous, tissue-specific functions of peripheral circadian rhythms. The function of circadian rhythms, however, will depend on the maturity of organoids, because previous studies

indicated lack of circadian rhythms in PSCs and mouse fetus during the early stages of its development (Reppert & Schwartz, 1986; Dierickx *et al*, 2017; Umemura *et al*, 2019). Therefore, we first characterized robustness of circadian rhythms from iPSCs to HIOs demonstrating the lack of robust circadian rhythms in HIOs. Differentiation of mouse embryonic or induced pluripotent stem cells results in the onset of circadian oscillations after 28 days (Umemura *et al*, 2017). Interestingly, a subsequent study from the same group found that human iPSCs require up to 90 days of differentiation to initiate circadian oscillations (Umemura *et al*, 2019). On the other hand, differentiation of human embryonic stem cells (ESC) into cardiomyocytes results in rhythmic cultures oscillations after 30 days. However, it is worth indicating that circadian oscillations of *Bmal1-dLuc* and *Per2-dLuc* reporter activities in the differentiated cardiomyocytes show weak oscillations (Dierickx *et al*, 2017)
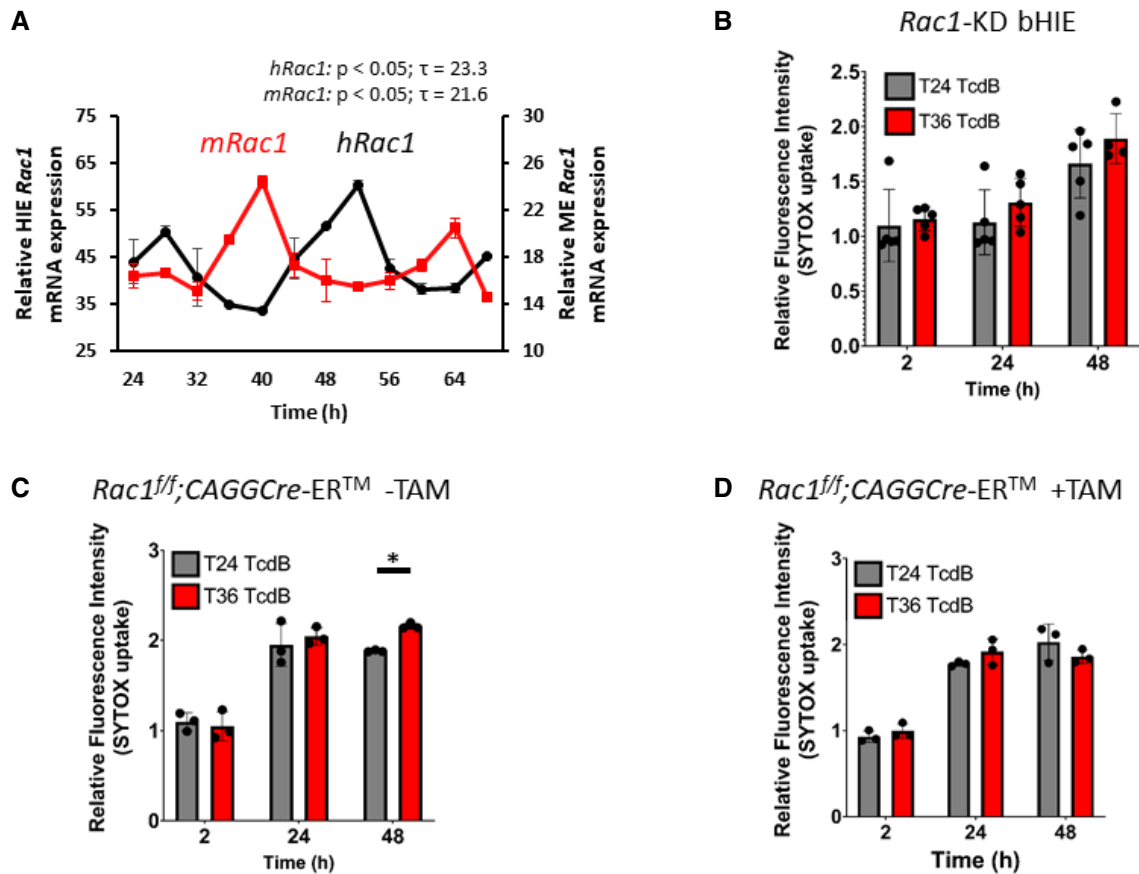
Figure 6. Disruption of *Rac1* abolishes circadian time-dependent necrotic cell death responses.

A   Validation of anti-phasic *Rac1* expression in mouse (*mRac1*, red) and human enteroids (*hRac1*, black) by qRT–PCR.

B   Quantitative analysis of fluorescent intensity from SYTOX orange in *Rac1*-KD bHIEs.

C, D   Quantitative analysis of fluorescent intensity from SYTOX orange in control *Rac1* ^f/f^;CAGGCre-ER^TM^ *without tamoxifen (C) or Rac1* ^f/f^;CAGGCre-ER^TM^ *with tamoxifen-treated (D) enteroids.*

Data information: Data represented as mean $\pm$ S.D. of $n = 5$ technical replicates. All of the data were normalized to time- and phase-matched vehicle controls set to 1.
*$P < 0.05$ (two-way ANOVA).

Source data are available online for this figure.

compared to HIEs (Fig 1B) and differentiated cells from iPSCs after 90 days of differentiation (Umemura *et al*, 2019). The lack of robust circadian rhythms in HIOs after 35-day differentiation protocol is consistent with the lack of circadian oscillations at day 42 of *in vitro* differentiation of human iPSCs by Umemura and colleagues (Umemura *et al*, 2019), which indicate that further maturation is necessary for the development of circadian rhythms.

In contrast to HIOs, we observe robust circadian rhythms in both kcHIEs and bHIEs based on their identical bioluminescence outputs and oscillations reflecting the activity of *Bmal1-luc* reporter (Fig 1B). However, we observe lower amplitude of *Bmal1*, *Per2,* and *Rev-erbα* transcripts in kcHIEs compared to bHIEs (Fig 2E). These findings suggest that kcHIEs represent an intermediate state between HIOs and bHIEs, which is in agreement with previous results (Watson *et al*, 2014; Finkbeiner *et al*, 2015). Transcriptomic analysis comparing HIOs, kcHIEs, and adult intestinal tissue demonstrated that kcHIEs possess intermediate expression of brush border enzymes, *sucrase isomaltase* and *trehalase*, between HIOs and adult intestinal tissue (Watson *et al*, 2014). Similar findings were discovered for expression profiles of Paneth and stem cell markers in HIOs, kcHIEs, vs. adult intestinal tissue (Finkbeiner *et al*, 2015). It would be interesting to perform RNA-Seq using time course samples from kcHIEs to compare and contrast CCGs between kcHIEs and bHIEs characterizing the reorganization of CCGs during development.

Approximately 3–10% of transcriptome show circadian oscillations in mouse enteroids and bHIEs regulating diverse signaling pathways ranging from cell cycle to immune response. It is not clear why we observe a lower number of CCGs in mouse enteroids compared to bHIEs, but the number of cycling genes in both mouse and human enteroids indicate that these *in vitro* systems possess functional circadian rhythms regulating a large number of tissue-specific CCGs. In contrast, NIH3T3 and U2OS cells show less than a dozen cycling genes despite the presence of robust core clock gene oscillations (Hughes *et al*, 2009). On the other hand, 3–16% of cycling genes are observed depending on peripheral organs of mice *in vivo* (Zhang *et al*, 2014*)*. We hypothesize that intestinal epithelial

cells *in vivo* will show a greater number of CCGs compared to enteroids, because those CCGs will be a result of both systemic cues and peripheral circadian clocks. In our future work, we plan to compare CCGs in mouse enteroids and mouse intestinal tissue to systematically dissect CCGs that are controlled by systemic cues and intestinal clocks.

The intestinal circadian clock possesses robust circadian rhythms (Moore *et al*, 2014) and is responsible for promoting circadian variation in a wide range of biological processes (Rosselot *et al*, 2016), including intestinal motility (Kumar *et al*, 1986), nutrient absorption (Pan & Hussain, 2009), innate immunity (Froy & Chapnik, 2007), timing of cell division (Matsu-ura *et al*, 2016), and the pathogenic response (Bellet *et al*, 2013). In patients, nocturnal diarrhea is an "alarm" symptom that should prompt clinicians to consider further evaluation, including testing for *C. difficile* infection (Cohen *et al*, 2010). However, whether a disrupted circadian clock predisposes to or is a result of gastrointestinal infections remains largely unknown. Insights to such questions will be needed to determine whether or not targeting circadian rhythms to treat such diseases would be efficacious. Our findings demonstrate robust operation of canonical clock genes regulating specific signaling pathways, and species-dependent anti-phasic expression of *Rac1* between mouse and human enteroids explaining the observed anti-phasic necrotic cell death response in mouse vs. human enteroids against TcdB. It is intriguing that we observe anti-phasic expression of *Rac1* between mouse and human enteroids despite similar phases of canonical clock genes (Fig 5C). We speculate that this could be due to either different accessibility and/or transcriptional regulation of the *Rac1* promoter between mouse and human enteroids. In the future, we plan to evaluate the importance of circadian-phase specific expression of *Rac1* and other genes that are involved in signaling by RHO GTPases between mouse and human enteroids, and design chronotherapeutic regimens for treatments of *C. difficile* infection. Furthermore, our work demonstrates a proof of concept that human organoids derived from different organs and disease states could provide a unique opportunity to: (i) characterize function of peripheral circadian clocks in different organs, (ii) identify circadian biomarkers for human diseases, and (iii) leverage the information to develop novel circadian treatment regimens for translational applications.

Materials and Methods

Animals

Mouse enteroids were established and cultured from 3- to 6–month-old C57BL/6J (Jackson Laboratories), PER2::LUCIFERASE (Yoo *et al*, 2004), and *Bmal1*$^{f/f}$-*EsrCRE* (Yang *et al*, 2016). We generated a conditional *Rac1*-KO mouse (*Rac1*$^{f/f}$;CAGGCre-ER^{TM}) by crossing *Rac1*$^{f/f}$ (Stock No: 005550, Jackson Laboratory) and tamoxifen-inducible CAGGCre-ER^{TM} (Stock No: 034795, Jackson Laboratory) mice. Immune-deficient NSG mice (Jackson Laboratories) were utilized for kidney capsule transplantation of HIOs (Watson *et al*, 2014). Animal handling was performed according to IACUC protocols #2016-0014 (PI: Michael Helmrath—Cincinnati Children's Hospital Medical Center) and #17-01-30-01 (PI: Christian Hong—University of Cincinnati).

Isolation and maintenance of mouse enteroids

Mouse jejunal enteroids were generated following established protocols (Nalapareddy *et al*, 2017). Briefly, crypt domains from small intestinal tissue were isolated, added to 40 μl of Matrigel (Corning) membrane matrix, suspended as a single 3D Matrigel dome within a 24-well plate, and provided 400 μl mouse enteroid media (Advanced DMEM/F-12 (Gibco), L-Glutamine (Gibco), Penicillin/Streptomycin (Gibco), N-2 (Gibco), B-27 (Gibco), 10 mM HEPES solution (Millipore-Sigma), 50 ng/ml recombinant murine EGF (Peprotech), and R-Spondin/Noggin conditioned media generated in-house. Enteroids were passaged every 4–7 days via a 27G syringe (BD). CRE-driven *Bmal1* exon 4 or *Rac1* exon 1 excisions were initiated *in vitro* by adding 1 μM 4-OH tamoxifen (Cayman) for 24-h to *Bmal1*$^{f/f}$-*EsrCRE* or *Rac1*$^{f/f}$;CAGGCre-ER^{TM} enteroids. All samples were maintained in cell culture incubators set at 37°C and 5% CO$_2$. Enteroids isolated from separate mice were considered biological replicate samples.

Experiment design to test for a circadian phase-dependent response to TcdB

1–2 HIOs and ≈15–20 mouse/human enteroids were plated per well to control for density. 100 nM dexamethasone (DEX) was added to treatment groups either 36 h (T36) or 24 h (T24) prior to TcdB addition. Samples were then exposed to a vehicle buffer (50 mM Tris Base Ultrapure (US biological), 100 mM NaCl (Fisher Scientific), pH 7.5) or *Clostridium difficile* toxin B (List Laboratories) by addition to cell culture media. SYTOX Orange (500 nM) (Invitrogen) was added with Vehicle/TcdB for quantification of necrotic cell death. Four wells of a 24-well plate were seeded with twenty enteroids/well at the onset of each experiment. Five enteroids within each well were randomly selected for imaging. These same five enteroids were imaged at 2, 24, and 48 h post-vehicle/TcdB addition on a Dmi8 inverted microscope (Leica Microsystems) to minimize the confounding variable of imaging different enteroids at each time point. When quantifying fluorescence from SYTOX™ Orange, an area of interest was manually traced around each enteroid using LasX software from Leica microsystems. An independent area of interest was generated for each enteroid at each time point to account for enteroid growth during the experiment. Fluorescence intensity within the area of interest was reported by the LasX imaging software. This approach was selected to minimize the variability in overall size of each enteroid. A total of 20 individual enteroids (5 technical replicates from 4 biological replicates) were analyzed for each treatment group. All TcdB data were set relative to time- and phase-matched vehicle controls set to 1.

HIO generation

Human intestinal organoids were generated following previously established protocols (Spence *et al*, 2011) using multiple pluripotent stem cell (PSC) lines (Table EV2). Briefly, PSCs were differentiated through the definitive endoderm stage via the addition of Activin A (Cell Guidance Systems) between day-0 (D0) and D2, BMP4 (R&D Systems) at D1 and CHIR99021 (Stemgent)/FGF4 (R&D Systems) from D3 to D6. The addition of CHIR99021/FGF4 prompted the formation of midgut tube spheroids from the definitive endoderm

monolayer. At D7 midgut tube spheroids were collected and suspended in a Matrigel dome (Corning). Spheroids were then grown in gut media: DMEM/F12 (Gibco) supplemented with N-2 (Gibco), B-27 (Gibco), HEPES solution (Millipore-Sigma), recombinant murine epidermal growth factor (Peprotech), L-Glutamine (Gibco), Penicillin/Streptomycin (Gibco). At D21, sample density was reduced to $\approx$1–3 per 50 µl Matrigel bubble. Samples were grown for an additional 14 days in gut media, resulting in terminal HIO cultures (Spence *et al*, 2011). Individual HIOs were considered as biological replicates for all experiments. All experimentation using human tissues described herein was approved by an IRB at CCHMC (IRB#2014-0427). Informed consent for tissue collection, storage, and use of the samples was obtained from the donors at CCHMC.

Generation and maintenance of kidney capsule-matured and biopsy-derived human intestinal enteroids

Human intestinal organoids were transplanted into the kidney capsule of immune-deficient NOD-SCID IL-2Rγ^{null} (NSG) (Jackson Laboratories) mice, as previously described (Watson *et al*, 2014). Crypt domains from transplanted HIOs were isolated and suspended in Matrigel domes to form kidney capsule-matured human intestinal enteroids (kcHIEs; Mahe *et al*, 2015). Biological replicates for kcHIEs are derived from the human crypts harvested from three independent mice. Four independent frozen duodenal patient biopsy-derived human intestinal enteroids (bHIEs) were provided by the lab of Dr. Noah Shroyer (Baylor College of Medicine, Table EV2). Both bHIEs and kcHIEs were cultured following identical protocols. Enteroids were expanded by suspending pelleted enteroids in Matrigel and plating as three separate 10 µl domes/well in a 24-well plate. Intesticult organoid growth medium (StemCell Technologies) was used for enteroid expansion. Human enteroid differentiation was initiated by replacing expansion media with differentiation (Intesticult Component A (StemCell Technologies) mixed at a 1:1 ratio with DMEM/F12 supplemented with 15 mM HEPES) media 2 days post-passaging. Human enteroids were maintained in differentiation media at least four days before being used for experiments. kcHIEs derived from separate transplanted mice were counted as biological replicates. bHIEs isolated from separate human patient biopsies were counted as biological replicates.

Bmal1-luciferase lentiviral transduction and monitoring of bioluminescence

All human samples from PSCs to HIOs, kcHIEs and bHIEs were transduced with the same pABpuro-BluF (Addgene) plasmid DNA (Brown *et al*, 2005). Plasmid DNA was packaged into lentiviral vectors by the Viral Vector Core at Cincinnati Children's Hospital Medical Center (CCHMC). PSC transduction was carried out following a previously published lentiviral transduction protocol (Matsuura *et al*, 2016). Transduced PSCs were Puromycin selected (2 µg/ml) (Invivogen) and differentiated into definitive endoderm (DE) and midgut tube (MG) cultures, generating PSC, DE, and MG clock reporting samples. Midgut tube samples were re-transduced following the same protocol used for PSC transduction and differentiated into HIOs to generate *Bmal1-luc* reporting HIOs. The bHIE and kcHIE transduction protocol was designed by merging previously reported enteroid digestion (Zou *et al*, 2017) and transduction (Koo

et al, 2012) protocols. After transduction, digested enteroids were suspended in Matrigel and plated following normal culture protocol. 350 µl of Intesticult Component A/B (1:1) media supplemented with 10 µM ROCK inhibitor and 10 µM CHIR99021 was added to the culture. After 24 h, the media was replaced with 350 µl Intesticult Component A/B (1:1) supplemented with 10 µM ROCK inhibitor. On day two post-infection, media was transitioned to Intesticult Component A/B (1:1) supplemented with 2 µg/ml Puromycin. Puromycin selection was maintained for 2 weeks before starting experiments. *Bmal1-luc* transduced samples were monitored for clock output over 4-days with a KronosDIO luminometer (ATTO). PSC, DE, MG, and HIO samples were maintained in normal culture media throughout recording. kcHIEs and bHIEs were differentiated for 4 days prior to bioluminescence recording. On day 4, samples were re-plated to 35 mm dishes, synchronized and added to the KronosDIO to begin recording. All samples were provided a 1-hour clock synchronization stimulus with 100 nM DEX (Millipore-Sigma) and given new, non-DEX containing, media prior to recording. 200 µM Luciferin (GoldBio) was added to each culture for luminescence detection.

Time course sample collection

Rhythmic gene expression was determined via time course sample collection. Samples were collected every 4 h over a 48-h period, two full circadian cycles. At each collection time point, cells were pelleted, suspended in 1 ml TRI reagent (Molecular Research Center) and snap-frozen in liquid N_2. After completion of the time course, RNA was isolated via a RNeasy mini-kit column (Qiagen) and cDNA were generated using the Superscript III Reverse transcriptase kit (Invitrogen). FAST SYBR green (Applied Biosystems) and gene-specific primer pairs were used to quantify gene expression via real-time quantitative reverse transcriptase polymerase chain reaction (qRT–PCR) with TATA-Box Binding protein (*Tbp*) expression used as a housekeeping gene.

FACS analysis

A quantitative assessment of apoptosis and necrosis in mouse enteroids and bHIEs was performed using fluorescein isothiocyanate (FITC) Annexin V Apoptosis Detection Kit I (BD Pharmingen). Enteroids were dissociated using TrypLE for ~5 min at 37°C to get single cells ($0.5 \sim 1 \times 10^6$ cells). The crypt suspension was washed with 1 ml of DMEM/F12 medium and centrifuged down. Pellets were resuspended in 100 µl PBS by mixing 5 µl of FITC-conjugated Annexin V (Annexin V-FITC) and 5 µl propidium iodide (PI) according to manufacturer's instructions. The cells were incubated for 15 min at room temperature in the dark. The stained cells were diluted with 400 µl binding buffer and immediately analyzed by the BD FACSCalibur flow cytometer (BD Biosciences, Heidelberg, Germany). 10,000 cells were analyzed per measurement. Data were processed using the CellQuestPro Software (Kwan *et al*, 2016; Natarajan *et al*, 2019). Dose–response curves were used to determine different concentrations of TcdB for mouse and human intestinal enteroids (Appendix Fig S4A and B).

RNA-sequencing analysis

To perform RNA-sequencing, we collected C57BL/6J mouse enteroids and human bHIEs derived from patient sample #103

(Table EV2) as a time course. Mouse enteroids were pooled from two separate mice to mitigate single mouse biasing and bHIEs were from a single patient (female, 24-years old) biopsy. Samples were collected every two hours for 46 h starting at 24 h post-DEX synchronization. Isolated RNA samples were shipped on dry ice for further processing and sequencing analysis using paired-end reads with 50 million reads per sample by Novogene. Raw RNA-sequencing FASTQ files were directly used to generate expression files using the Kallisto (Bray *et al*, 2016) embedded algorithm inside the Altanalyze module (Emig *et al*, 2010). Kallisto pseudo-aligned each transcript with the Ensemble reference transcriptome (Ensembl version 72) and calculated TPM (transcripts per million) by Altanalyze (Emig *et al*, 2010). For PSEA, we used the reference gene sets in c2.cp.v5.0.symbols.gmt downloaded from the Molecular Signatures Database (MSigDB).

Statistical analysis

All data are displayed as mean values of at least three biological replicates with error bars representing standard deviation around the mean. KronosDIO bioluminescent traces were quantified for clock parameters via fast Fourier transformation (Matsu-ura *et al*, 2016). qRT–PCR and RNA-seq transcript expression profiles were tested for significant rhythms using the R package MetaCycle 2D (Wu *et al*, 2016; *P*-value cutoff of 0.05; Thaben & Westermark, 2014). All between-group comparisons were made using a two-way analysis of variance (two-way ANOVA) with Tukey's post hoc analysis. Normality of the residuals was confirmed with Shapiro's test of residuals at a significance of $P < 0.05$. All statistical tests were performed in R Studio version 1.2.1335.

Data availability

RNA-Seq data are available at the Gene Expression Omnibus (GEO, GSE179028) following the link below. https://www.ncbi.nlm.nih.gov/geo/query/acc.cgi?acc=GSE179028.

Expanded View for this article is available online.

Author contributions

AER, MP, and MK designed the experiments, collected the data, generated, and compiled figures and wrote the manuscript. TM-U and SL assisted in designing and performing experiments. KRS, KC, and NSa received and aligned RNA-sequencing data to reference transcriptomes. DEF, GW, and JBH analyzed RNA-sequencing data and generated the associated figures. NSu and JAH performed surgical transplantation of HIOs into the kidney capsule of mice and provided kcHIEs. TRB provided HIOs and assisted in the design of HIO related experiments. HAM provided kcHIE samples. NFS supplied bHIEs and reviewed the manuscript. MAH, JMW, and JBH were involved in the study design and review of this manuscript. SRM and CIH designed and directed the overall progress of studies, wrote and provided final approval of the manuscript.

Conflict of interest

The authors declare that they have no conflict of interest.

References

Abt MC, McKenney PT, Pamer EG (2016) *Clostridium difficile* colitis: pathogenesis and host defence. *Nat Rev Microbiol* 14: 609–620

Barca-Mayo O, Pons-Espinal M, Follert P, Armirotti A, Berdondini L, De Pietri TD (2017) Astrocyte deletion of *Bmal1* alters daily locomotor activity and cognitive functions via GABA signalling. *Nat Commun* 8: 14336

Bellet MM, Deriu E, Liu JZ, Grimaldi B, Blaschitz C, Zeller M, Edwards RA, Sahar S, Dandekar S, Baldi P *et al* (2013) Circadian clock regulates the host response to *Salmonella. Proc Natl Acad Sci* 110: 9897–9902

Best EL, Freeman J, Wilcox MH (2012) Models for the study of *Clostridium difficile* infection. *Gut Microbes* 3: 145–167

Brancaccio M, Patton AP, Chesham JE, Maywood ES, Hastings MH (2017) Astrocytes control circadian timekeeping in the suprachiasmatic nucleus via glutamatergic signaling. *Neuron* 93: 1420–1435.e5

Bray NL, Pimentel H, Melsted P, Pachter L (2016) Near-optimal probabilistic RNA-seq quantification. *Nat Biotechnol* 34: 525–527

Brown SA, Fleury-Olela F, Nagoshi E, Hauser C, Juge C, Meier CA, Chicheportiche R, Dayer J-M, Albrecht U, Schibler U (2005) The period length of fibroblast circadian gene expression varies widely among human individuals. *PLoS Biol* 3: e338

Buffie CG, Jarchum I, Equinda M, Lipuma L, Gobourne A, Viale A, Ubeda C, Xavier J, Pamer EG (2012) Profound alterations of intestinal microbiota following a single dose of clindamycin results in sustained susceptibility to *Clostridium difficile*-induced *colitis. Infect Immun* 80: 62–73

Buhr ED, Vemaraju S, Diaz N, Lang RA, Van Gelder RN (2019) Neuropsin (OPN5) mediates local light-dependent induction of circadian clock genes and circadian photoentrainment in exposed murine skin. *Curr Biol* 29: 3478–3487

Chen P, Tao L, Wang T, Zhang J, He A, Lam KH, Liu Z, He X, Perry K, Dong M *et al* (2018) Structural basis for recognition of frizzled proteins by *Clostridium difficile* toxin B. *Science* 360: 664–669

Clevers H (2016) Modeling development and disease with organoids. *Cell* 165: 1586–1597

Cohen SH, Gerding DN, Johnson S, Kelly CP, Loo VG, McDonald LC, Pepin J, Wilcox MH (2010) Clinical practice guidelines for *Clostridium difficile* infection in adults: 2010 update by the society for healthcare epidemiology of America (SHEA) and the Infectious Diseases Society of America (IDSA). *Infect Control Hosp Epidemiol* 31: 431–455

Crosby P, Hamnett R, Putker M, Hoyle NP, Reed M, Karam CJ, Maywood ES, Stangherlin A, Chesham JE, Hayter EA *et al* (2019) Insulin/IGF-1 drives PERIOD synthesis to entrain circadian rhythms with feeding time. *Cell* 177: 896–909

Damiola F, Le Minh N, Preitner N, Kornmann B, Fleury-Olela F, Schibler U (2000) Restricted feeding uncouples circadian oscillators in peripheral tissues from the central pacemaker in the suprachiasmatic nucleus. *Genes Dev* 14: 2950–2961

Dierickx P, Vermunt MW, Muraro MJ, Creyghton MP, Doevendans PA, van Oudenaarden A, Geijsen N, Van Laake LW (2017) Circadian networks in human embryonic stem cell-derived cardiomyocytes. *EMBO Rep* 18: 1199–1212

Edgar RS, Stangherlin A, Nagy AD, Nicoll MP, Efstathiou S, O'Neill JS, Reddy AB (2016) Cell autonomous regulation of herpes and influenza virus infection by the circadian clock. *Proc Natl Acad Sci* 113: 10085–10090

Emig D, Salomonis N, Baumbach J, Lengauer T, Conklin BR, Albrecht M (2010) AltAnalyze and DomainGraph: analyzing and visualizing exon expression data. *Nucleic Acids Res* 38: W755–W762

Farrow MA, Chumbler NM, Lapierre LA, Franklin JL, Rutherford SA, Goldenring JR, Lacy DB (2013) *Clostridium difficile* toxin B-induced necrosis is mediated by the host epithelial cell NADPH oxidase complex. *Proc Natl Acad Sci* 110: 18674–18679

Finkbeiner SR, Hill DR, Altheim CH, Dedhia PH, Taylor MJ, Tsai Y-H, Chin AM, Mahe MM, Watson CL, Freeman JJ (2015) Transcriptome-wide analysis reveals hallmarks of human intestine development and maturation *in vitro* and *in vivo*. *Stem Cell Reports* 4: 1140–1155

Forbester JL, Goulding D, Vallier L, Hannan N, Hale C, Pickard D, Mukhopadhyay S, Dougan G (2015) Interaction of *Salmonella enterica* serovar Typhimurium with intestinal organoids derived from human induced pluripotent stem cells. *Infect Immun* 83: 2926–2934

Froy O, Chapnik N (2007) Circadian oscillation of innate immunity components in mouse small intestine. *Mol Immunol* 44: 1954–1960

Guillaumond F, Dardente H, Giguère V, Cermakian N (2005) Differential control of *Bmal1* circadian transcription by REV-ERB and ROR nuclear receptors. *J Biol Rhythms* 20: 391–403

Guo H, Brewer JM, Champhekar A, Harris RBS, Bittman EL (2005) Differential control of peripheral circadian rhythms by suprachiasmatic-dependent neural signals. *Proc Natl Acad Sci* 102: 3111–3116

Hill DR, Huang S, Nagy MS, Yadagiri VK, Fields C, Mukherjee D, Bons B, Dedhia PH, Chin AM, Tsai Y-H *et al* (2017) Bacterial colonization stimulates a complex physiological response in the immature human intestinal epithelium. *Elife* 6: e29132

Hughes ME, DiTacchio L, Hayes KR, Vollmers C, Pulivarthy S, Baggs JE, Panda S, Hogenesch JB (2009) Harmonics of circadian gene transcription in mammals. *PLoS Genet* 5: e1000442

Just I, Selzer J, Wilm M, Von Eichel-Streiber C, Mann M, Aktories K (1995) Glucosylation of Rho proteins by *Clostridium difficile* toxin B. *Nature* 375: 500–503

Kelly CP, Pothoulakis C, LaMont JT (1994) *Clostridium difficile* colitis. *N Engl J Med* 330: 257–262

Kiessling S, Dubeau-Laramée G, Ohm H, Labrecque N, Olivier M, Cermakian N (2017) The circadian clock in immune cells controls the magnitude of Leishmania parasite infection. *Sci Rep* 7: 1–11

Koo B-K, Stange DE, Sato T, Karthaus W, Farin HF, Huch M, van Es JH, Clevers H (2012) Controlled gene expression in primary *Lgr5* organoid cultures. *Nat Methods* 9: 81–83

Kowalska E, Moriggi E, Bauer C, Dibner C, Brown SA (2010) The circadian clock starts ticking at a developmentally early stage. *J Biol Rhythms* 25: 442–449

Kretzschmar K, Clevers H (2016) Organoids: modeling development and the stem cell niche in a dish. *Dev Cell* 38: 590–600

Kumar D, Wingate D, Ruckebusch Y (1986) Circadian variation in the propagation velocity of the migrating motor complex. *Gastroenterology* 91: 926–930

Kwan YP, Saito T, Ibrahim D, Al-Hassan FMS, Ein Oon C, Chen Y, Jothy SL, Kanwar JR, Sasidharan S (2016) Evaluation of the cytotoxicity, cell-cycle arrest, and apoptotic induction by Euphorbia hirta in MCF-7 breast cancer cells. *Pharmaceutical Biology* 54: 1223–1236

Lee C, Etchegaray J-P, Cagampang FR, Loudon AS, Reppert SM (2001) Posttranslational mechanisms regulate the mammalian circadian clock. *Cell* 107: 855–867

Leslie JL, Huang S, Opp JS, Nagy MS, Kobayashi M, Young VB, Spence JR (2015) Persistence and toxin production by *Clostridium difficile* within human intestinal organoids result in disruption of epithelial paracellular barrier function. *Infect Immun* 83: 138–145

Mahe MM, Sundaram N, Watson CL, Shroyer NF, Helmrath MA (2015) Establishment of human epithelial enteroids and colonoids from whole tissue and biopsy. *J Vis Exp* e52483

Matsu-ura T, Dovzhenok A, Aihara E, Rood J, Le H, Ren Y, Rosselot AE, Zhang T, Lee C, Obrietan K *et al* (2016) Intercellular coupling of the cell cycle and circadian clock in adult stem cell culture. *Mol Cell* 64: 900–912

Moore SR, Pruszka J, Vallance J, Aihara E, Matsuura T, Montrose MH, Shroyer NF, Hong CI (2014) Robust circadian rhythms in organoid cultures from PERIOD2:LUCIFERASE mouse small intestine. *Dis Model Mech* 7: 1123–1130

Mukherji A, Kobiita A, Ye T, Chambon P (2013) Homeostasis in intestinal epithelium is orchestrated by the circadian clock and microbiota cues transduced by TLRs. *Cell* 153: 812–827

Nagoshi E, Saini C, Bauer C, Laroche T, Naef F, Schibler U (2004) Circadian gene expression in individual fibroblasts: cell-autonomous and self-sustained oscillators pass time to daughter cells. *Cell* 119: 693–705

Nalapareddy K, Nattamai KJ, Kumar RS, Karns R, Wikenheiser-Brokamp KA, Sampson LL, Mahe MM, Sundaram N, Yacyshyn M-B, Yacyshyn B *et al* (2017) Canonical Wnt signaling ameliorates aging of intestinal stem cells. *Cell Rep* 18: 2608–2621

Natarajan U, Venkatesan T, Radhakrishnan V, Samuel S, Rathinavelu A (2019) Differential mechanisms of cell death induced by HDAC inhibitor SAHA and MDM2 inhibitor RG7388 in MCF-7 cells. *Cells* 8: 8

Nayak G, Zhang KX, Vemaraju S, Odaka Y, Buhr ED, Holt-Jones A, Kernodle S, Smith AN, Upton BA, D'Souza S *et al* (2020) Adaptive thermogenesis in mice is enhanced by Opsin 3-dependent adipocyte light sensing. *Cell Rep* 30: 672–686

Noel G, Baetz NW, Staab JF, Donowitz M, Kovbasnjuk O, Pasetti MF, Zachos NC (2017) A primary human macrophage-enteroid co-culture model to investigate mucosal gut physiology and host-pathogen interactions. *Sci Rep* 7: 1–14

Pan X, Hussain MM (2009) Clock is important for food and circadian regulation of macronutrient absorption in mice. *J Lipid Res* 50: 1800–1813

Pando MP, Morse D, Cermakian N, Sassone-Corsi P (2002) Phenotypic rescue of a peripheral clock genetic defect via SCN hierarchical dominance. *Cell* 110: 107–117

Papatheodorou P, Zamboglou C, Genisyuerek S, Guttenberg G, Aktories K (2010) Clostridial glucosylating toxins enter cells via clathrin-mediated endocytosis. *PLoS One* 5: e10673

Preitner N, Damiola F, Lopez-Molina L, Zakany J, Duboule D, Albrecht U, Schibler U (2002) The orphan nuclear receptor REV-ERBα controls circadian transcription within the positive limb of the mammalian circadian oscillator. *Cell* 110: 251–260

Reineke J, Tenzer S, Rupnik M, Koschinski A, Hasselmayer O, Schrattenholz A, Schild H, von Eichel-Streiber C (2007) Autocatalytic cleavage of *Clostridium difficile* toxin B. *Nature* 446: 415–419

Reischl S, Vanselow K, Westermark PO, Thierfelder N, Maier B, Herzel H, Kramer A (2007) β-TrCP1-mediated degradation of PERIOD2 is essential for circadian dynamics. *J Biol Rhythms* 22: 375–386

Reppert S, Schwartz W (1986) Maternal suprachiasmatic nuclei are necessary for maternal coordination of the developing circadian system. *J Neurosci* 6: 2724–2729

Rosselot AE, Hong CI, Moore SR (2016) Rhythm and bugs: circadian clocks, gut microbiota, and enteric infections. *Curr Opin Gastroenterol* 32: 7–11

Ruben MD, Wu G, Smith DF, Schmidt RE, Francey LJ, Lee YY, Anafi RC, Hogenesch JB (2018) A database of tissue-specific rhythmically expressed human genes has potential applications in circadian medicine. *Sci Transl Med* 10: eaat8806

Sato TK, Panda S, Miraglia LJ, Reyes TM, Rudic RD, McNamara P, Naik KA, FitzGerald GA, Kay SA, Hogenesch JB (2004) A functional genomics strategy reveals Rora as a component of the mammalian circadian clock. *Neuron* 43: 527–537

Saxena K, Blutt SE, Ettayebi K, Zeng X-L, Broughman JR, Crawford SE, Karandikar UC, Sastri NP, Conner ME, Opekun AR *et al* (2016) Human intestinal enteroids: a new model to study human rotavirus infection, host restriction, and pathophysiology. *J Virol* 90: 43–56

Schibler U, Gotic I, Saini C, Gos P, Curie T, Emmenegger Y, Sinturel F, Gosselin P, Gerber A, Fleury-Olela F *et al* (2015) Clock-talk: interactions between central and peripheral circadian oscillators in mammals. *Cold Spring Harb Symp Quant Biol* 80: 223–232

Schmalen I, Reischl S, Wallach T, Klemz R, Grudziecki A, Prabu JR, Benda C, Kramer A, Wolf E (2014) Interaction of circadian clock proteins CRY1 and PER2 is modulated by zinc binding and disulfide bond formation. *Cell* 157: 1203–1215

Siepka SM, Yoo S-H, Park J, Song W, Kumar V, Hu Y, Lee C, Takahashi JS (2007) Circadian mutant Overtime reveals F-box protein FBXL3 regulation of cryptochrome and period gene expression. *Cell* 129: 1011–1023

Silver R, LeSauter J, Tresco PA, Lehman MN (1996) A diffusible coupling signal from the transplanted suprachiasmatic nucleus controlling circadian locomotor rhythms. *Nature* 382: 810–813

Sinagoga KL, McCauley HA, Múnera JO, Reynolds NA, Enriquez JR, Watson C, Yang H-C, Helmrath MA, Wells JM (2018) Deriving functional human enteroendocrine cells from pluripotent stem cells. *Development* 145: dev165795

Sinturel F, Gos P, Petrenko V, Hagedorn C, Kreppel F, Storch K-F, Knutti D, Liani A, Weitz C, Emmenegger Y *et al* (2021) Circadian hepatocyte clocks keep synchrony in the absence of a master pacemaker in the suprachiasmatic nucleus or other extrahepatic clocks. *Genes Dev* 35: 329–334

Spence JR, Mayhew CN, Rankin SA, Kuhar MF, Vallance JE, Tolle K, Hoskins EE, Kalinichenko VV, Wells SI, Zorn AM *et al* (2011) Directed differentiation of human pluripotent stem cells into intestinal tissue *in vitro*. *Nature* 470: 105–109

Stokkan K-A, Yamazaki S, Tei H, Sakaki Y, Menaker M (2001) Entrainment of the circadian clock in the liver by feeding. *Science* 291: 490–493

Thaben PF, Westermark PO (2014) Detecting rhythms in time series with RAIN. *J Biol Rhythms* 29: 391–400

Thaiss CA, Levy M, Korem T, Dohnalová L, Shapiro H, Jaitin DA, David E, Winter DR, Gury-BenAri M, Tatirovsky E *et al* (2016) Microbiota diurnal rhythmicity programs host transcriptome oscillations. *Cell* 167: 1495–1510

Thaiss C, Zeevi D, Levy M, Zilberman-Schapira G, Suez J, Tengeler A, Abramson L, Katz M, Korem T, Zmora N *et al* (2014) Transkingdom control of microbiota diurnal oscillations promotes metabolic homeostasis. *Cell* 159: 514–529

Tso CF, Simon T, Greenlaw AC, Puri T, Mieda M, Herzog ED (2017) Astrocytes regulate daily rhythms in the suprachiasmatic nucleus and behavior. *Curr Biol* 27: 1055–1061

Umemura Y, Koike N, Matsumoto T, Yoo S-H, Chen Z, Yasuhara N, Takahashi JS, Yagita K (2014) Transcriptional program of Kpna2/Importin-α2 regulates cellular differentiation-coupled circadian clock development in mammalian cells. *Proc Natl Acad Sci* 111: E5039–E5048

Umemura Y, Koike N, Ohashi M, Tsuchiya Y, Meng QJ, Minami Y, Hara M, Hisatomi M, Yagita K (2017) Involvement of posttranscriptional regulation of Clock in the emergence of circadian clock oscillation during mouse development. *Proc Natl Acad Sci* 114: E7479–E7488

Umemura Y, Maki I, Tsuchiya Y, Koike N, Yagita K (2019) Human circadian molecular oscillation development using induced pluripotent stem cells. *J Biol Rhythms* 34: 525–532

Watson CL, Mahe MM, Múnera J, Howell JC, Sundaram N, Poling HM, Schweitzer JI, Vallance JE, Mayhew CN, Sun Y *et al* (2014) An *in vivo* model of human small intestine using pluripotent stem cells. *Nat Med* 20: 1310

Wells JM, Spence JR (2014) How to make an intestine. *Development* 141: 752–760

Welz P-S, Zinna VM, Symeonidi A, Koronowski KB, Kinouchi K, Smith JG, Guillén IM, Castellanos A, Furrow S, Aragón F *et al* (2019) BMAL1-driven tissue clocks respond independently to light to maintain homeostasis. *Cell* 177: 1436–1447

Wu G, Anafi RC, Hughes ME, Kornacker K, Hogenesch JB (2016) MetaCycle: an integrated R package to evaluate periodicity in large scale data. *Bioinformatics* 32: 3351–3353

Yagita K, Horie K, Koinuma S, Nakamura W, Yamanaka I, Urasaki A, Shigeyoshi Y, Kawakami K, Shimada S, Takeda J *et al* (2010) Development of the circadian oscillator during differentiation of mouse embryonic stem cells *in vitro*. *Proc Natl Acad Sci* 107: 3846–3851

Yang G, Chen L, Grant GR, Paschos G, Song W-L, Musiek ES, Lee V, McLoughlin SC, Grosser T, Cotsarelis G *et al* (2016) Timing of expression of the core clock gene *Bmal1* influences its effects on aging and survival. *Sci Transl Med* 8: 324ra16

Yoo S-H, Mohawk JA, Siepka SM, Shan Y, Huh SK, Hong H-K, Kornblum I, Kumar V, Koike N, Xu M *et al* (2013) Competing E3 ubiquitin ligases govern circadian periodicity by degradation of CRY in nucleus and cytoplasm. *Cell* 152: 1091–1105

Yoo S-H, Yamazaki S, Lowrey PL, Shimomura K, Ko CH, Buhr ED, Siepka SM, Hong H-K, Oh WJ, Yoo OJ *et al* (2004) PERIOD2:LUCIFERASE real-time reporting of circadian dynamics reveals persistent circadian oscillations in mouse peripheral tissues. *Proc Natl Acad Sci* 101: 5339–5346

Zhang R, Lahens NF, Ballance HI, Hughes ME, Hogenesch JB (2014) A circadian gene expression atlas in mammals: Implications for biology and medicine. *Proc Natl Acad Sci* 111: 16219–16224

Zhang R, Podtelezhnikov AA, Hogenesch JB, Anafi RC (2016) Discovering biology in periodic data through phase set enrichment analysis (PSEA). *J Biol Rhythms* 31: 244–257

Zou WY, Blutt SE, Crawford SE, Ettayebi K, Zeng X-L, Saxena K, Ramani S, Karandikar UC, Zachos NC, Estes MK (2017) Human intestinal enteroids: new models to study gastrointestinal virus infections. *Methods Mol Biol* 1576: 229–247